PLANT COMMISSIONING TEST TO VERIFY DYNAMIC STABILITY PHENOMENON IN CANDU 600 MWe PRIMARY CIRCUIT

S. ALIKHAN*, W. S. PILKINGTON*, W. J. GARLAND**

* New Brunswick Electric Power Commission
P.O. Box 10, Lepreau N.B. Canada
E0G 2H0

** Previously with Atomic Energy of Canada Limited, presently with Department of Engineering Physics, McMaster University, Hamilton, Ontario, Canada, L8S 4M1

PRESENTED AT THE INSTITUTION OF NUCLEAR ENGINEERS CONFERENCE ON SIMULATION FOR NUCLEAR REACTOR TECHNOLOGY, CAMBRIDGE, ENGLAND, APRIL 9-11, 1984.

INTRODUCTION

The complex phenomenon of flow oscillations in a two phase flow systems has been well studied since early 1960's. A detailed analysis and classification of these mechanisms can be readily found in the open literature(1).

The phenomenon of dynamic instability in Candu heat transport system was first identified by Atomic Energy of Canada Limited (AECL) in the latter stages of design when performing code simulation studies to analyse system response to imposed asymmetric disturbances (2). New simplified analytical models were developed to provide in-depth understanding of the physical mechanisms and cross-checking of the code predictions. These efforts were supplemented by a detailed experimental program at the Whiteshell Nuclear Research Establishment (WRNE-AECL) and Westinghouse Canada under the joint cooperation of AECL, and Ontario Hydro.

The computer code, SOPHT, (Simulation Of Primary Heat Transport) was tuned to the "as-built" plant conditions to enable good prediction of the single phase steady state and transient test data. Having developed the required degree of confidence in the Code, a series of runs were done to characterize the instability phenomenon with various amounts of steam quality in the outlet header. Several design solutions were then studied in order to achieve the required degree of stability in response to the worst possible asymmetric system disturbance. An optimized solution consisted of connecting the two reactor outlet headers in each loop through a suitably designed interconnect pipe.

The design fix was backfitted in the field during early stages of commissioning but was not placed in service until after field tests confirmed the nature and extent of the instability. Subsequent to the successful field demonstration of instability and excellent comparison of the test data with the code predictions, the interconnect was placed in service. Further dynamic testing for instability confirmed that the oscillatory behaviour following asymmetric disturbances was convergent under the "worst-case" transient and therefore the problem was demonstrated to have been resolved.

This paper describes the mechanism of the instability phenomenon, the analytical techniques used to predict the characteristic dynamic behaviour, field testing carried out to fine-tune the analytical code in order to enable good prediction of the steady state and transient single phase data, and the on-power dynamic tests with net steam quality in the reactor outlet headers to verify the phenomenon.

CANDU 600 HEAT TRANSPORT SYSTEM

Figure 1 gives an overview of the CANDU Primary Heat transport System. The core of a CANDU reactor is contained within a low pressure tank called the calandria as shown in figures 2 and 3. The fuel channel assemblies run through the calandria and contain the bundles of natural uranium fuel. The calandria is filled with heavy water (D_2O) which moderates or slows the fast neutrons, making a chain reaction possible. The heat of fission generated within the fuel is removed by the pressurized heavy water coolant which is pumped through the fuel channels. This hot coolant is passed through the steam generator where heat is transferred to light water to generate steam.

The pressure tube forms the pressure boundary of the Heat Transport System (HTS) in the core the heavy water coolant passes through and around the bundles of natural uranium fuel located within the pressure tube. A calandria tube surrounds each pressure tube and is in contact with the moderator. The annular space between the pressure tube and the calandria tube provides thermal insulation between the hot heat transport system coolant and the cool moderator.

The portions of the fuel channel assemblies external to the calandria are known as the end fittings; the end fittings are connected to the feeder pipes which feed coolant into and out of the fuel channels.

The CANDU 600 reactor has 380 fuel channels arranged in a square lattice within the calandria. The Heat Transport System (HTS) is arranged into two circuits, one on each side of the vertical centre line of the reactor core, with 190 fuel channels in each circuit. Figure 4 shows an end view of the arrangement of the main components of the HTS.

Each Heat Transport Circuit contains 2 pumps, 2 steam generators, 2 inlet headers and 2 outlet headers in a "figure-of-eight" arrangement. Feeders connect the inlet and outlet of the fuel channels to the inlet and outlet headers respectively.

The flow through the fuel channels is bi-directional (i.e. opposite directions in adjacent channels). The feeders are sized such that the coolant flow to each channel is approximately proportional to channel power. The enthalpy increase of the coolant is therefore approximately the same for each fuel channel assembly.

The operating pressure of the CANDU 600 reactor (outlet header) is 9.89 MPa(g). In order to increase unit efficiency, boiling in the core at high power is utilized, leading to a design outlet header quality of up to approximately 4% at full power. Other typical Heat Transport System parameters are given in Figure 1. Because of a combination of design conservations in pumps, steam generators and lack of design fouling on heat transfer surfaces, the actual net steam quality in reactor outlet headers at nominal full power is close to zero. Net quality will of course exist under transient operating conditions resulting from over-power, reduction in system pressure, flow etc.

To enhance Heat Transport System stability, a small pipe (150 mm I.D.) has been added to each circuit and is now an integral part of the system design. This pipe connects the reactor outlet on one side of the core to the reactor outlet on the other side of the core, as shown in Figures 5.

The Heat Transport System pressure is controlled by the Pressurizer. On falling pressure the 5-200 kW electrical heaters are switched on in proportion to the pressure error. On rising pressure, the steam above the saturated D_2O liquid is bled to the Degasser Condenser through the steam bleed valves. The inventory of the Pressurizer is controlled by feed and bleed valves to maintain constant system inventory. The pressurizer level is programmed as a function of power in order to accommodate for swell as reactor power is raised from zero power hot condition to full power.

INSTABILITY PHENOMENON (2,3)

The CANDU reactor design are inherently stable for single and parallel channel modes of instability since the single phase to two phase pressure drop ratio is high for the feeder-channel-feeder flow path between reactor inlet and outlet headers. There is however the possibility of a overall circuit oscillation of the process parameters due to compound dynamic instability under the following conditions.

a) void in both ends of the "figure-of-eight" circuit.
b) low inherent system damping.
c) presence of an asymmetric disturbance.

Given these conditions, the Heat Transport System would exhibit an oscillation with the following characteristics.

a) about a 14 second period related to transit time of density wave around the circuit.
b) sinusoidal flow variation in time with maximum amplitude occurring in single phase regions.
c) sinusoidal pressure variation in time with the maximum amplitude occuring in the two phase region.

In order to help understand the mechanism, the primary heat transport system is simplified as shown in figure 6 alongwith the single and two phase regions of a loop and its equivalent spring-mass model.

There are three dynamic effects interacting on the heat transport fluid following an asymmetric disturbance.

- the spring-mass effect
- the flow-enthalpy-pressure effect.
- the resistance losse effect.

With reference to figure 6, the two-phase regions (1-3 and 4-5) act like a spring (compressible) and single phase regions (3-4 and 6-1) act like masses (incompressible). Given a small pressure reduction at point 2, the fluid in upstream liquid region is accelerated and in the downstream region decelerated. The mass flow into the two phase region 1-3 is increased, thereby compressing the region and increasing its pressure. At the same time the other two phase region 4-6 under goes expansion. The inertia of the system causes the increase in flow to the perturbed region to continue even after the pressure has returned to normal. An overpressure will result causing a rebound effect. The upstream region now decelerates and downstream accelerates. In the absence of losses or gains, the oscillations will continue undiminished. The characteristic period for this effect is approximately 14 seconds, and the phase shift is 180° between the two headers.

A positive feedback occurs through interaction of the flow and channel power. Assuming power transferred to the coolant remains constant, an increase in upstream flow will reduce specific enthalpy of the two-phase region which reduces the quality and void fraction. This causes further pressure collapse in the two phase region 1-3. Thus the positive feedback to flow results in collapse of void in one two-phase region and an excursive increase in void in the other two-phase region.

The flow-enthalpy-pressure effect therefore provides the forcing feature while the spring-mass effect provides the rebound function.

The main stabilizing effect is the resistive loss in the circuit which would tend to oppose the changes in fluid velocities. In the Heat Transport System, the flow losses alone are not sufficient to provide adequate damping.

A snapshot of flow, pressure and void fraction at an instant in time "t" and t + 1/2 cycle is given in figure 7 at various points in the heat transport. This very simplistic illustration shows that maximum flow variations occur in the liquid regions and maximum pressure and void variations occur in the reactor outlet header region. Distribution within regions is deliberately omitted for clarity.

With the interconnect in place (figure 8), a perturbation at point 2 propagates as above except that the interconnect allows the fluid to move from the remote header to the perturbed header. This directly reduces the driving force for the liquid pass velocity changes. In addition, it helps to relieve the subsequent void increase (and pressure increase) at the remote header. It is important to note that the exact nature of the fluid transferred, steam a liquid, is not important. What is important is the amount of volume moved and the timing of that movement.

For maximum effectiveness, the flow in the interconnect should be in phase with the pressure difference between the two headers as much as possible. However fluid inertia in the line causes a phase shift and delays the initial movement of the fluid as well as carries it on longer than required. Increasing the interconnect resistance will increase the in-phase component but will lower the amount of fluid transferred. Hence the interconnect resistance needs to be tuned to optimize the effectiveness of the interconnect. It is more effective if inertia is low to begin with and therefore steam filled interconnect is preferable to a liquid filled line.

OVERVIEW OF THE ANALYSIS (2,3)

AECL studies indicated that, without the reactor outlet header interconnect, divergent flow oscillations would occur with a quality range of 1-8% in the reactor outlet header.

The "worst-case" perturbation would be an opening of the pressurizer steam bleed valve resulting in direct extraction of mass from the Reactor outlet header.

As a measure of margin to stability, a damping ratio of flow was defined as follows.

$$\zeta = \frac{-\ln(x)/2\pi}{\sqrt{1+[\ln(x)/2\pi]^2}} \simeq -\frac{\ln(x)}{2\pi} \quad \text{for } |\zeta| < 0.1$$

Where x is peak-to-peak attenuation of oscillation between successive periods.

Negative damping indicates divergent oscillation, positive indicates convergent and zero indicates sustained oscillation.

The analysis included comparison of SOPHT* with test loop results (RD12**) and simple analytical formulations. Following initial refinements on spatial and temporal convergence in numerical analysis, all analytical models compared well with the test loop results in predicting the period and damping ratio. All models indicated possible divergent flow oscillations without header-to-header interconnect. However there exists stabilizing features in real CANDU 600 systems e.g. multi-channel effects, turbulent mixing and diffusion in large pipes, which are not represented in any model and laboratory tests.

The calculated pressure, flow and void fraction at positions of maximum variations are plotted as a function of time in figures 9, 10 & 11 for an initiating disturbance of 200 kg/s mass extraction from an outlet header for 5 seconds. The process trips have been removed from these simulations to allow a study of the oscillations as they develop.

---

* SOPHT: Simulation of Primary Heat Transport System (4)

** RD12: A semi-scale CANDU Test loop using electrical heaters. The loop is located at the AECL, Whiteshell Nuclear Research Establishment in Manitoba, Canada.

Initially, the pressure drops in the header that is disturbed. The remote header remains unaffected due to physical separation by the liquid regions until some change in velocity of these liquid regions has taken place for the the remote header to "see" the perturbation. The period of the developed oscillation is 14 seconds or roughly 2 times the transit time for void propagation in the two-phase region. The two halves of the circuit are approximately 180° out-of-phase.

The flow oscillations start with an initial increase in velocity in the upstream liquid region and decrease in the downstream liquid region. The perturbation affect both sides simultaneously and almost symmetrically.

Ultimately, if the oscillations are allowed to grow undamped, the void would collapse in one end with twice nominal void in the opposite end. At this limit cycle, the flow oscillations would be bounded by roughly + 30% and -50% of normal flow. (In the real case, reactor trip would have occurred when flow dropped 20% below normal).

Analysis indicates that divergent oscillations only occur over a limited range of 1 to 8% quality. At or below zero quality, compressible regions do not exist while at higher qualities, the flow-enthalpy-pressure feedback gain decreases.

After considerable design studies, one 150 mm pipe per loop with 65 mm orifice at each end was chosen as the optimum design fix to provide stability for all operating transients. With the two compressible regions interconnected, a perturbation affecting one compressible region would be transmitted more directly to the opposite compressible region thereby reducing the disturbance to the flow in the liquid region.

Figure 12 shows typical loop flows following the reference perturbation, assuming homogeneous conditions in the interconnect the same quality as reactor outlet headers. It was found that the oscillations dampen from a 3% initial disturbance to less that ± 1% of flow in about 3 cycles.

POINT LEPREAU POWER RUN-UP AND ASSOCIATED SOPHT CODE TUNING

In order to enable meaningful code predictions it was necessary to fine-tune the design codes to the specific "as-commissioned" operating data. At Point Lepreau, it was an interative process whereby operating data was collected at the following operating conditions for the purpose of code tuning in successive stages:

- zero power cold condition with 4 pumps in service.
- zero power hot condition.
- on-power operation at 5% to full power.

At each stage, a complete set of 500 measurements were taken to compare steady state data with code predictions. At power levels above 90% FP, a careful analysis of fuel channel outlet temperatures indicated that the first channel went into boiling at 93% FP. At full power, the outlet headers were at zero steam quality compared to the nominal design value of 4%.

STABILITY TESTING PROGRAM

Considering that earlier code prediction showed a divergent oscillation threshold of around 1% quality (figure 16), it would appear that instability would not be a problem at power levels below 103% FP at nominal heat transport operating conditions. This was not however a comfortable situation in view of the uncertainties in code predictions as well as the fact that more steam quality could be generated in reactor outlet headers under the following conditions:

- transient conditions of overpower, low pressure, low flow.
- chronic fouling of heat transfer surface area with age.

The following course of action was therefore adopted:

a) demonstrate instability at 100% FP with interconnect out-of-service at 2% steam quality by operating the heat transport system at reduced pressure.
b) characterize the instability phenomenon with code predictions and determine the required orifice size for the interconnect piping for optimum damping.
c) place interconnect in-service with the optimum orifice and re-test as for (a) to demonstrate stable operation.

PROCEDURE FOR TEST WITHOUT INTERCONNECT

In order to achieve significant steam quality, the system pressure was reduced in small steps. At each stage, a reference perturbation was applied to observe system response for instability. An outline of the test procedure is given below:

a) At 100% FP and normal system pressure of 9.89 MPa(g), apply a reference perturbation by opening both steam bleed valves for 10 seconds to demonstrate stable operation.

b) Reduce pressure in steps of 0.1 MPa until net quality is detected in reactor outlet headers. Two methods were used to detect the on-set of quality.

   i) observing swell (pressurizer level) as a function of system pressure.
   ii) observing decrease in outlet header temperature as a function of pressure and comparing it with the thermodynamic saturation line using steam tables.

   Method (ii) proved more definitive as swell curve was not sharp enough at the transition point to boiling (figure 13)

c) Determine system pressure corresponding to 2% steam quality.

d) Reduce pressure in steps of 0.1MPa and apply the reference perturbation until diverse oscillations are characterized.

Following precautions were taken in order to obtain the pertinent test data without adversely affecting plant status.

- Pressure control was placed on manual in order that oscillations could develop to pre-defined limits without the interference from control function.

- Careful monitoring of reactor trips parameters (low core flow, low heat transport pressure) on CRT displays in order to avoid a plant trip during the test.

- Should any of the trip limits are approached, the reactor power would be reduced to 85% at 0.5% FP per second to remove quality from outlet headers thereby reverting back to stable operating regime.

For data collection, the following arrangement was set-up:

- a total of 9 CRT screens were dedicated to monitor 36 parametric trends (4 per screen).

- a complete set of 500 point data log via plant computers.

- for transient data to characterize oscillations, a Hewlett Packard model 9825A mini-computer was set up to record a 10 variable set every second. Recording all of the variables at essentially the same time allowed direct determination of the phase relationships.

TEST RESULTS WITHOUT INTERCONNECT

The test was carried out on April 15, 1983. The system proved stable at normal system pressure when reference perturbation was applied. As the system pressure was red ced in steps of 100 kPa, the onset of void was observed at 9.81 MPa(g). Subsequent perturbations were applied at 9.7 MPa(g) and 9.64 MPa(g) as shown in figure 14. At 9.71 MPa(g) as small stable oscillation was induced with a period of 14 seconds but the amplitude was too small to obtain a meaningful set of data. At 9.64 MPa(g), a similar perturbation produced slightly larger oscillation. In order to avoid pressure rise due to control action, the setpoint was dropped to 9.55 MPa(g). The oscillation began to diverge and developed gradually until peak-to-peak amplitude of 10% was reached. The test was then terminated by allowing system pressure to rise by placing all 5 x 200 kW Pressurizer heaters in service.

Example of the variables recorded using HP Data Logger are given in figure 15. Although signal-to-noise levels are significant, only RIH-ROH differential pressure wave form is distorted. As predicted, the inlet to outlet header differential pressures in pass A and B of loop 1 are 180° out-of-phase whereas ROH-ROH differential pressures in loops 1 and 2 are almost in phase. This figure also shows two channel flows in loops 1 and 2 but in pass A and B to be 180° out-of-phase as predicted.

Figure 16 and 17 show comparison of test measurements with SOPHT Code prediction after it was tuned to the 65% FP test data (4). The calculated damping ratio is plotted in figure 16 as a function of steam quality alongwith two test data from Lepreau. Figure 17 shows a superimposed channel flow (B14) oscillation measured during the test over the predicted response. In both cases, the agreement is extremely good. This demonstrates the level of confidence achieved in SOPHT code prediction inspite of its modelling limitations.

STABILITY TEST WITH INTERCONNECT

At Point Lepreau, the interconnect was placed in service in May 1983 during the annual outage. The stability test was however carried out at a sister CANDU 600 MWe plant, Gentilly-2, in Quebec, Canada on September 23, 1983 using a similiar procedure as described before. A target pressure of 9 MPa(g) was selected to obtain a steam quality of 3% in the outlet headers. SOPHT runs by AECL had predicted a maximum damping at this quality. (5)

Figure 18 shows the system response to reference steam bleed perturbation at pressures of 9.9 to 9.1 MPa(g) in five steps. In all cases, stable performance was exhibited. Predicted system response on system pressure and channel flows is compared with actual test result in figure 19. The measured channel flows have been enhanced in scale to show damped oscillations. In the case of pressure, it may be noted that the initial response following steam bleed perturbation is not adequately predicted by SOPHT due perhaps to modelling difficulties of the pressurizer vessel.

The results have shown beyond any doubt that the reactor outlet header interconnect has solved the divergent oscillation phenomenon inherent in the design CANDU 600 MWe primary heat transport system. The remaining stable oscillations in the process parameters are considered small enough to be not of any significance for practical purposes.

CONCLUSIONS

As a result of the comprehensive and thorough program of analytical studies, laboratory testing and on-power plant testing, it has been clearly demonstrated that:

- The original CANDU 600 MWe primary heat transport system (without the interconnect) was susceptible to divergent oscillations in the presence of asymmetric disturbance with sufficient steam quality in the reactor outlet headers.

- With the addition of a suitably designed 150 mm diameter interconnect between the two reactor outlet headers in each loop, the system has been demonstrated to be convergent under the worst possible asymmetric perturbation that can be applied to the system. The instability problem in CANDU 600 MWe heat transport system therefore stands resolved.

- SOPHT code predictions of the stability test results based the current "best estimate" of heat transport system conditions and using the "twin channel" core model compares reasonably well with plant tests in terms of damping ratio and oscillation period.

ACKNOWLEDGEMENTS

The authors would like to thank Atomic Energy of Canada Limited, the designer of CANDU 600, for developing the analytical model and the associated laboratory test data to formulate and understand the stability phenomenon. The field commissioning work was planned and conducted by NB Power under the technical guidance of AECL who were responsible for fine-tuning of the Code and designing the interconnect piping.

Specific mention should also be made of the contribution made by Ontario Hydro who participated in a joint task force with AECL to understand the stability phenomenon and develop the anlytical models.

Finally we would like to acknowledge the close cooperation between NB Power and Hydro Quebec in planning, coordination and execution of the stability testing program.

REFERENCES

1. J.A. Boure, A.E. Bergles, L.S. Tong "Review of Two Phase Flow Instability", ASME 71-HT-42, 1971.

2. B.R. Ajmera, W.G. Garland, V.G. Snell "600 MWe CANDU Heat Transport System Flow Stability" AECL Document TDS-XX-33100-440-001 September 1981.

3. W.G. Garland, P Gulshani, H.W. Hinds, A.R. Khan, V. Snell "CANDU 600 Heat Transport System Flow Stability" 10th Simulation Symposium on Reactor Dynamics and Plant Control, organized by Canadian Nuclear Society at Saint John , N.B., Canada April 9/10, 1984.

4. C.Y.F. Chang, J. Skears "SOPHT - a computer model for CANDU-PHWR Heat Transport Networks and their Control", Nuclear Technology, 35, October 1977.

5. C.K. Choo, "Point Lepreau - PHT Stability commissioning Test Analysis" AECL Report TDAI-351 Dec. 1983 (Draft).

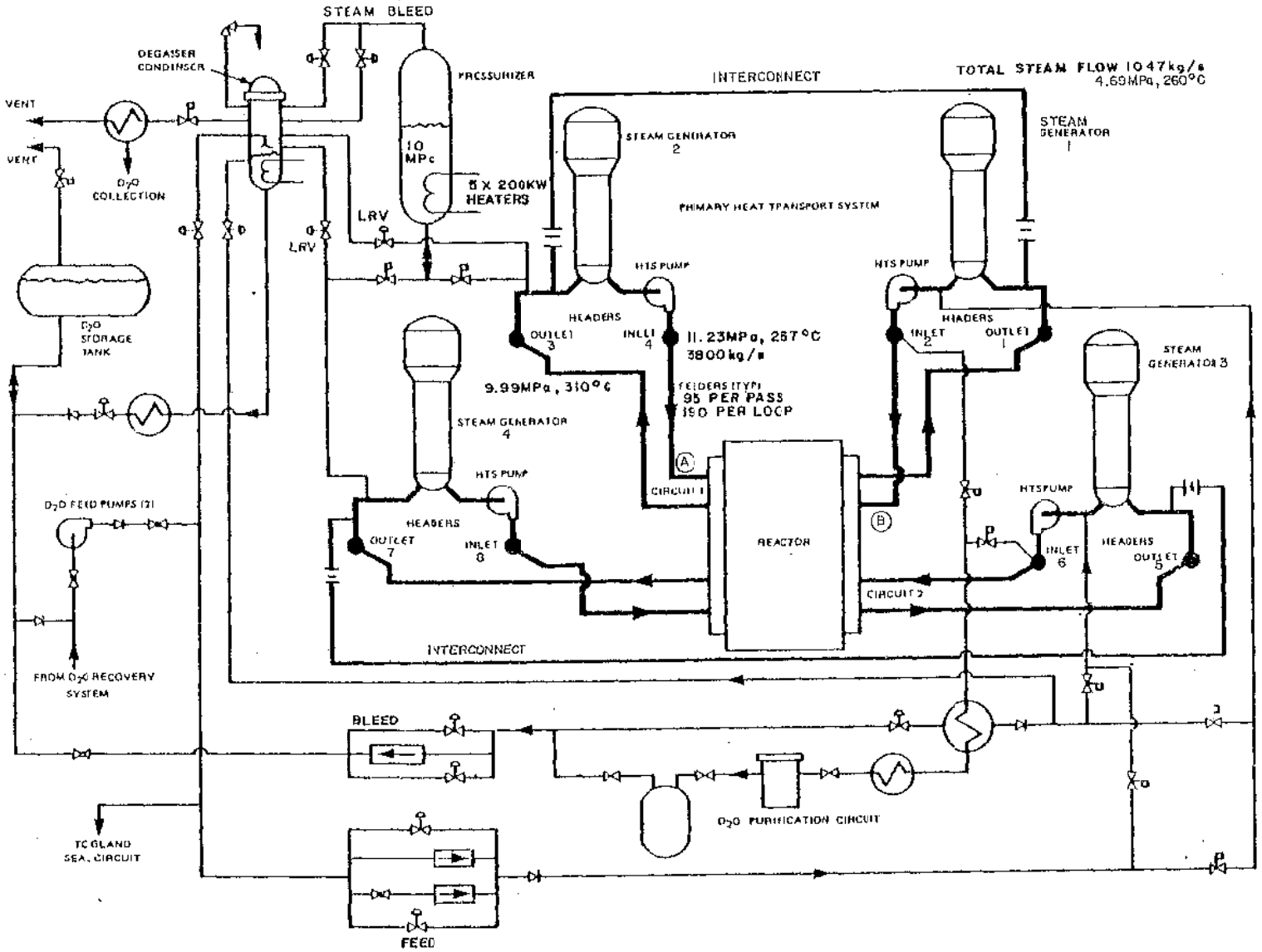

FIGURE 1 HEAT TRANSPORT SYSTEM NORMAL OPERATION FLOWSHEET

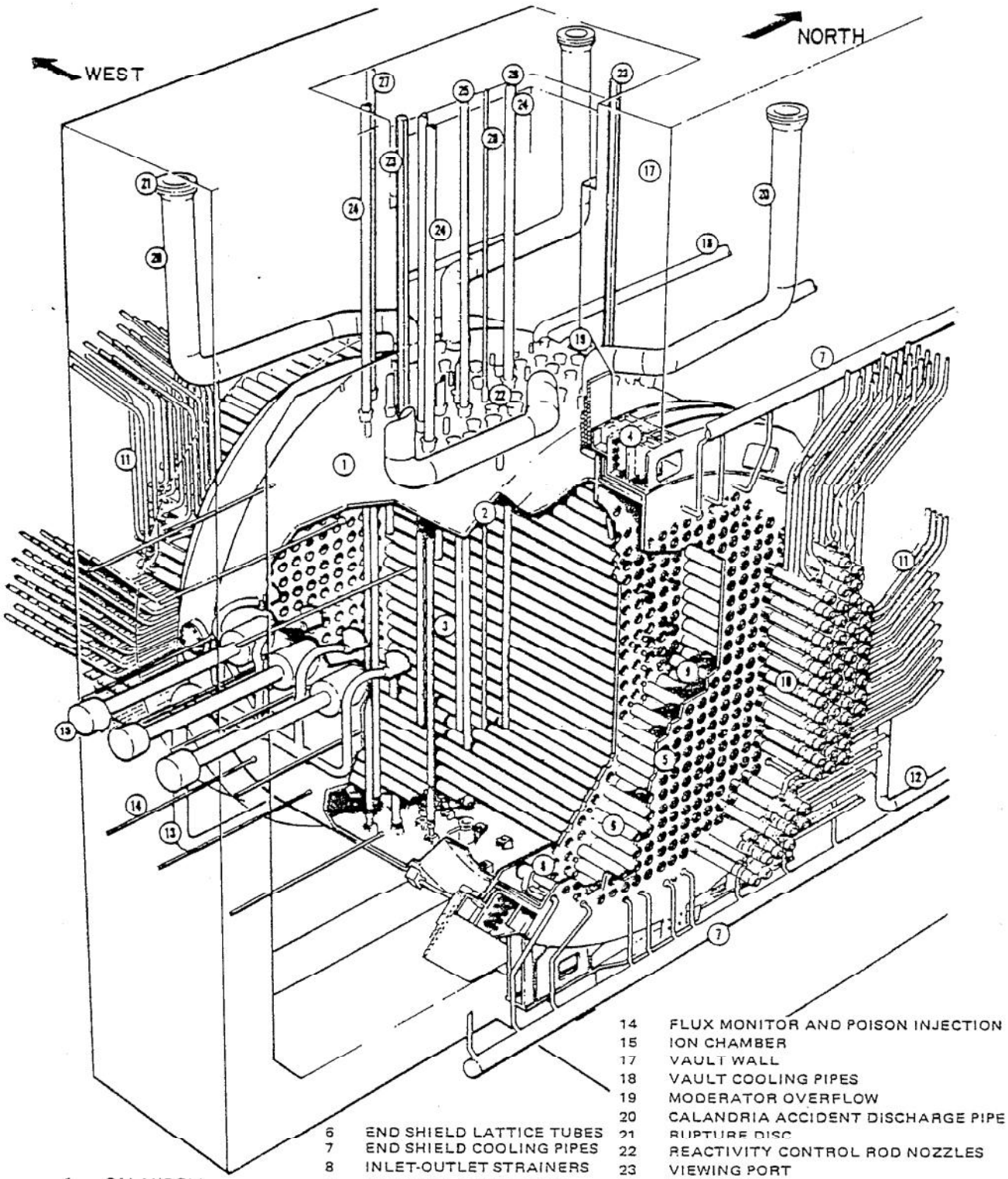

1 CALANDRIA
2 CALANDRIA SHELL
3 CALANDRIA TUBES
4 EMBEDMENT RING
5 FUELLING TUBESHEET
6 END SHIELD LATTICE TUBES
7 END SHIELD COOLING PIPES
8 INLET-OUTLET STRAINERS
9 STEEL BALL SHIELDING
10 END FITTINGS
11 FEEDER PIPES
12 MODERATOR OUTLET
13 MODERATOR INLET
14 FLUX MONITOR AND POISON INJECTION
15 ION CHAMBER
17 VAULT WALL
18 VAULT COOLING PIPES
19 MODERATOR OVERFLOW
20 CALANDRIA ACCIDENT DISCHARGE PIPE
21 RUPTURE DISC
22 REACTIVITY CONTROL ROD NOZZLES
23 VIEWING PORT
24 SHUTOFF ROD
25 ADJUSTER ROD
26 CONTROL ABSORBER ROD
27 ZONE CONTROL ROD
28 VERTICAL FLUX MONITOR

FIGURE 2 REACTOR ASSEMBLY

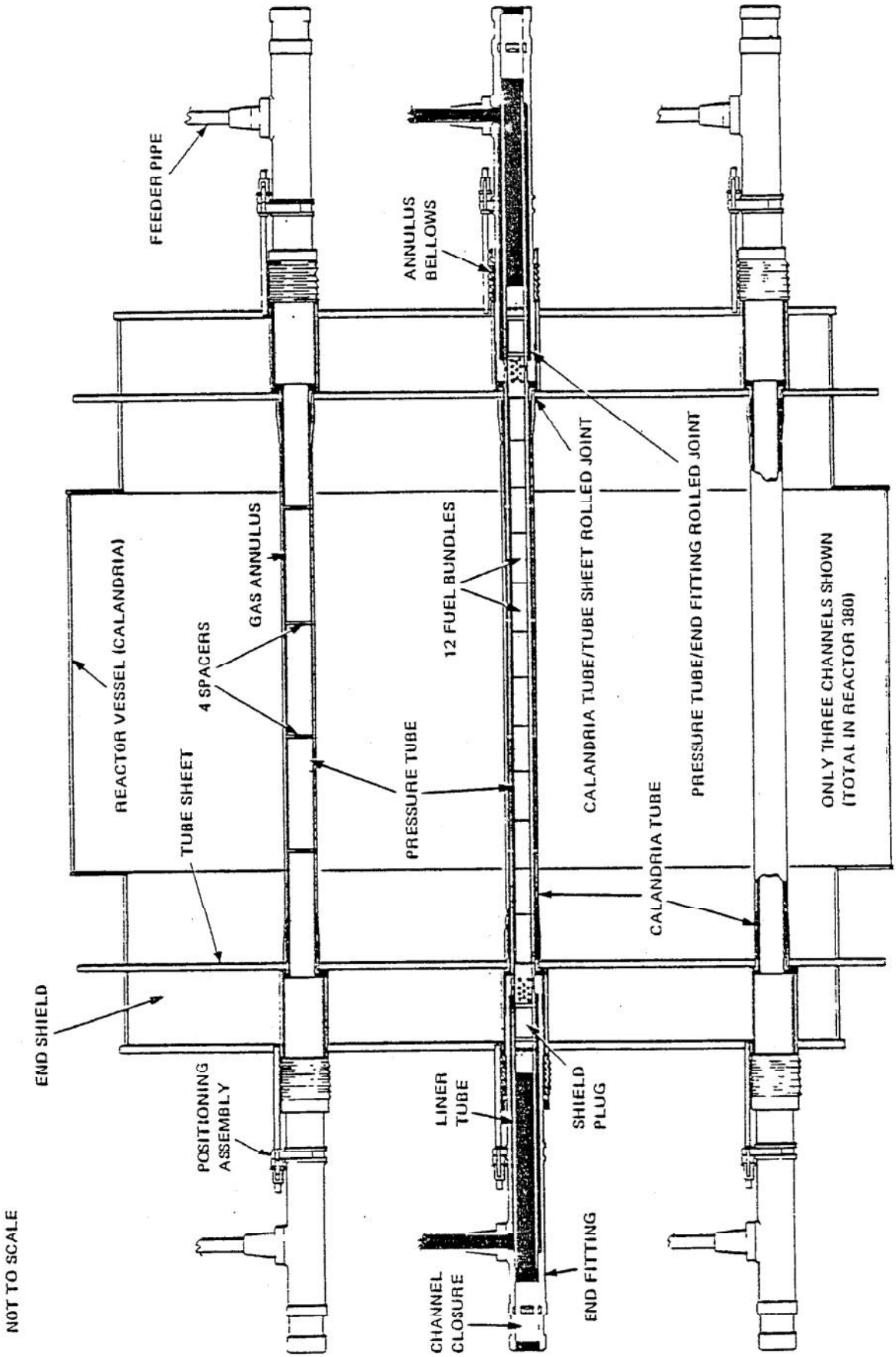

FIGURE 3 SIMPLIFIED DIAGRAM OF 600 MW REACTOR

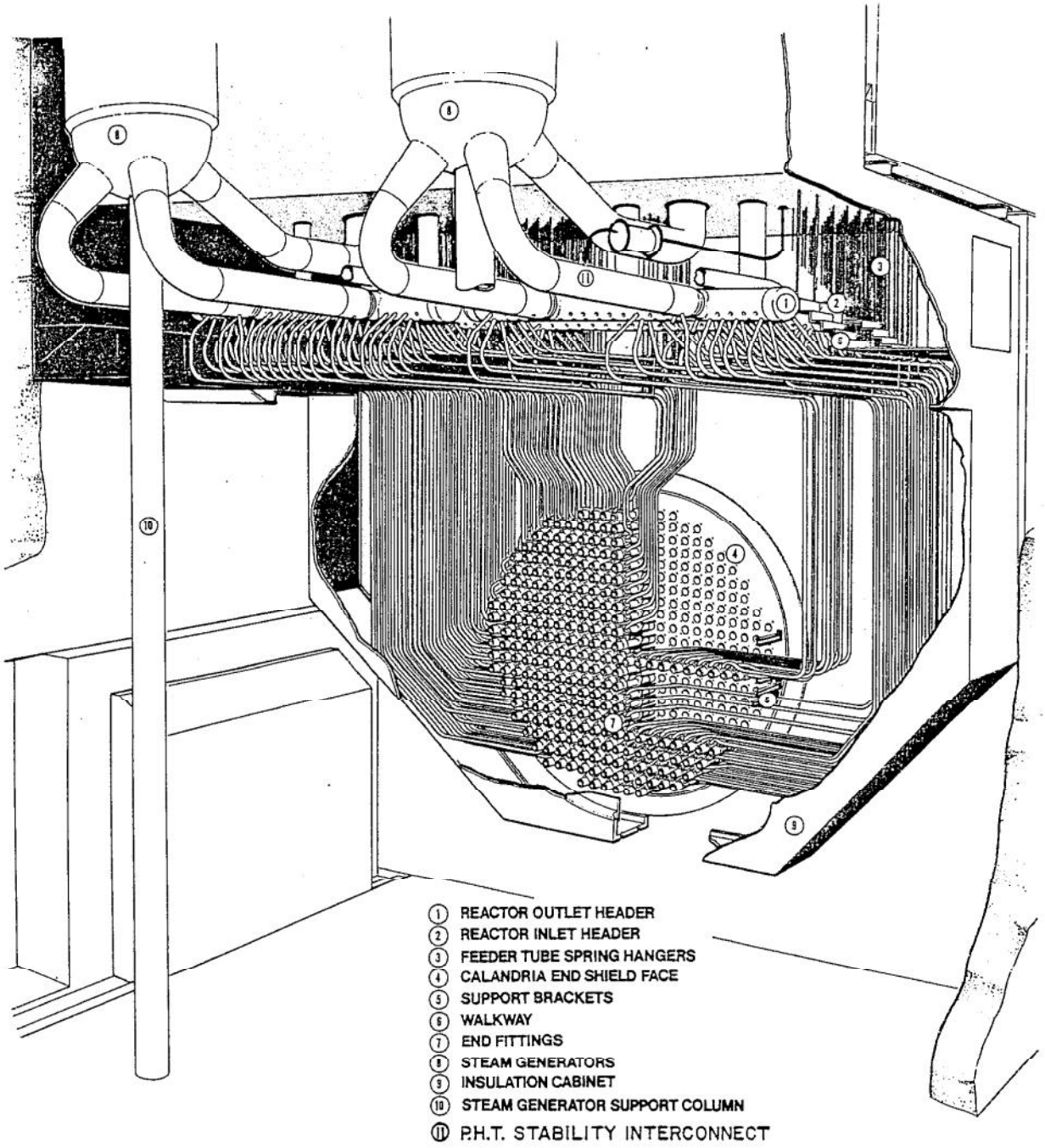

FIGURE 4 PRIMARY HEAT TRANSPORT SYSTEM TYPICAL FEEDER ARRANGEMENT

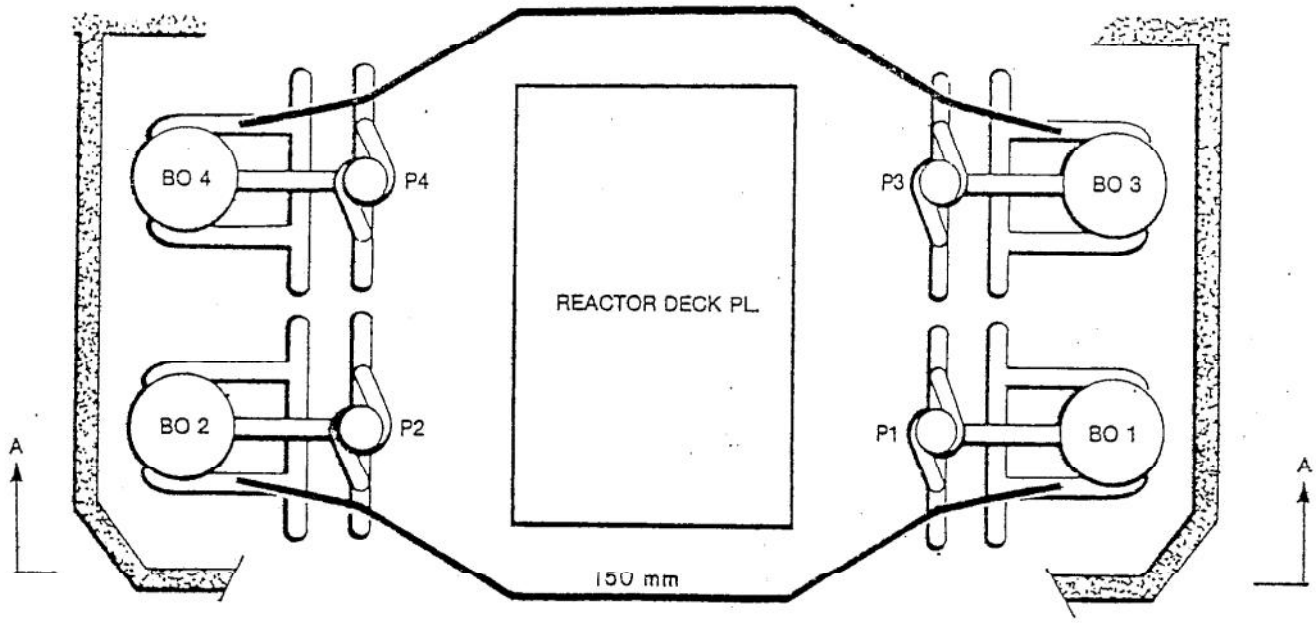

TOP VIEW

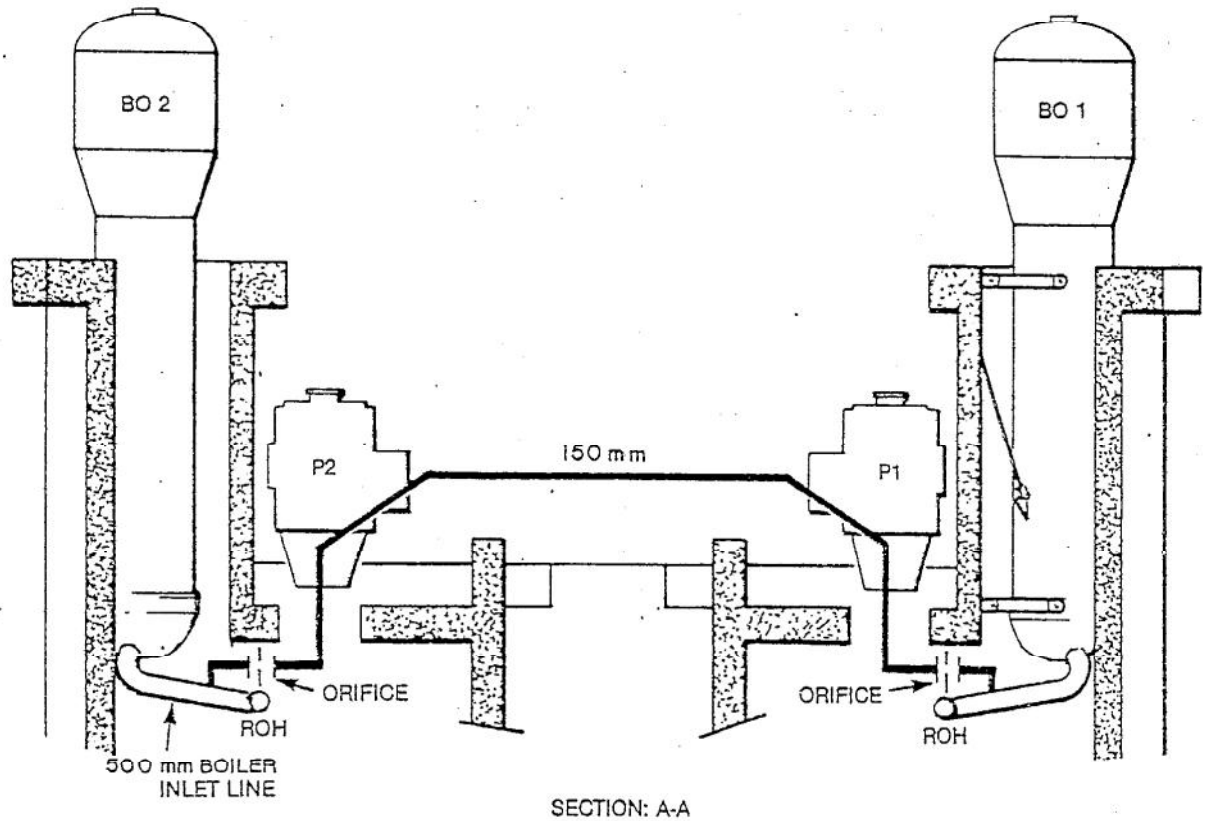

SECTION: A-A

FIGURE 5 PRIMARY HEAT TRANSPORT SYSTEM INSTABILITY FIX

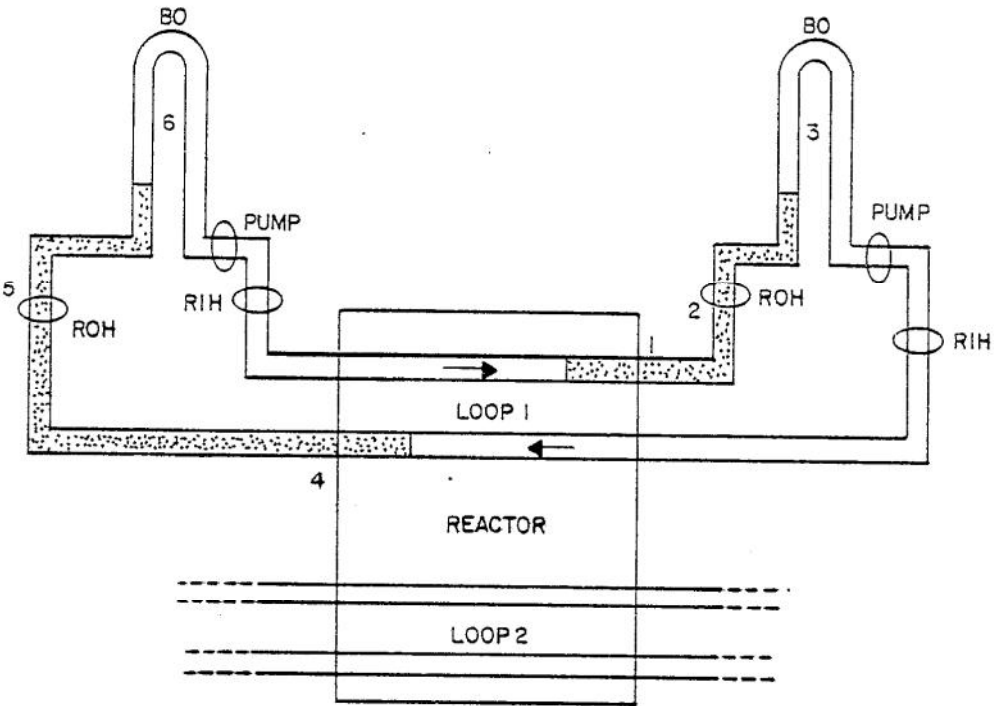

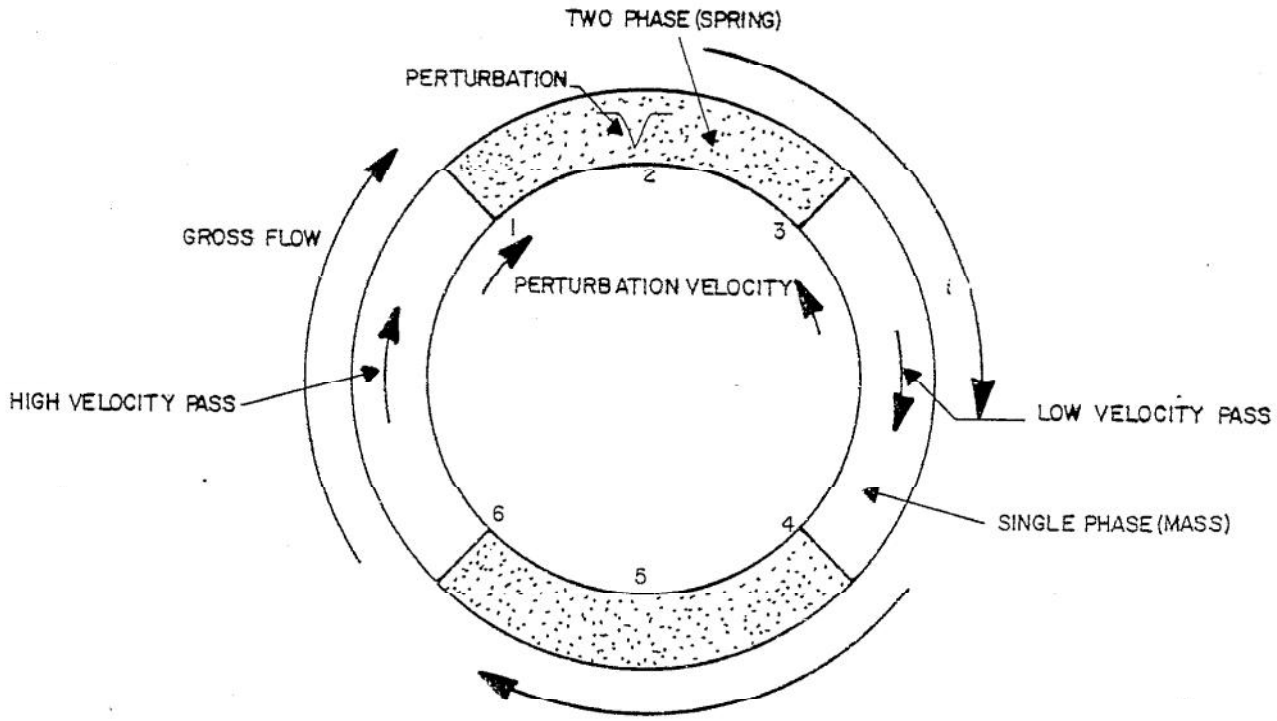

FIGURE 6 DYNAMIC OSCILLATORY BEHAVIOR – WITHOUT INTERCONNECT

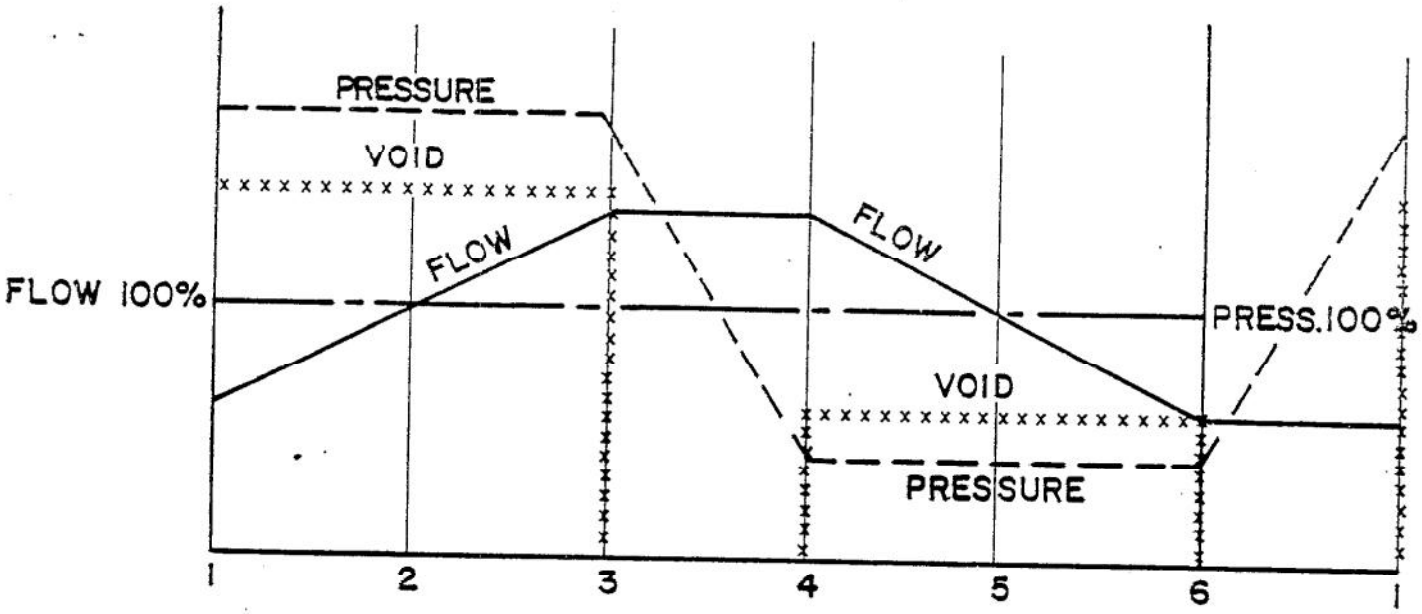

SNAPSHOT OF FLOW AND PRESSURE AT AN INSTANT IN TIME, t FOR VARIOUS POSITIONS (AS PER FIGURE 6)

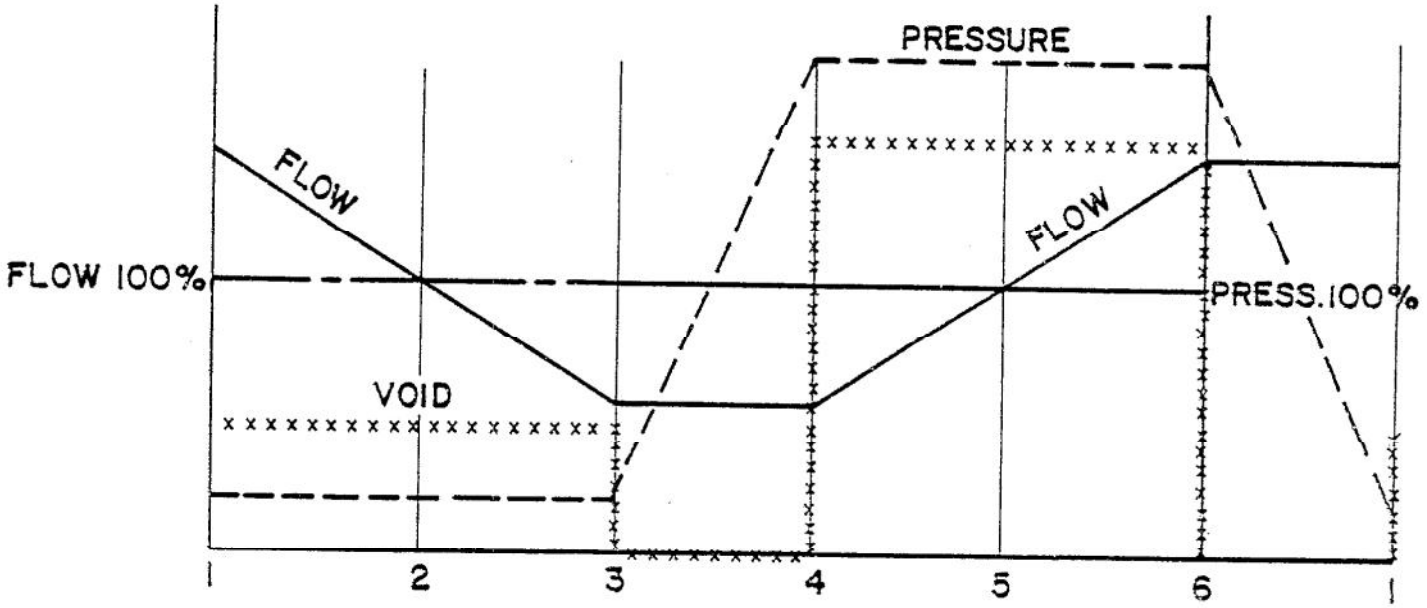

FIGURE 7 SNAPSHOT OF FLOW AND PRESSURE AT TIME (t + 1/2 CYCLE) FOR VARIOUS POSITIONS (AS PER FIGURE 6)

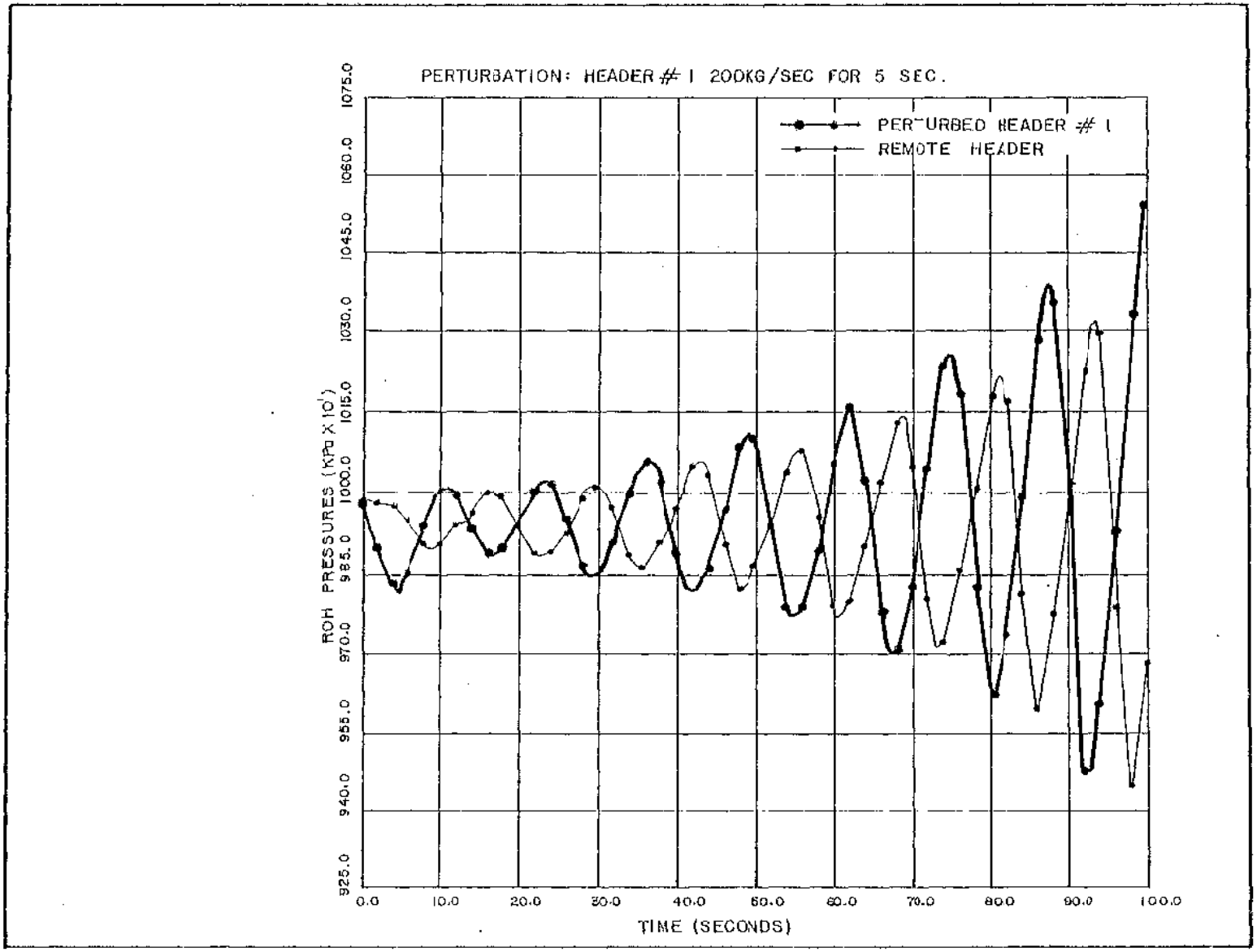

FIGURE 9 REACTOR OUTLET HEADER, PRESSURE vs. TIME
NO INTERCONNECT

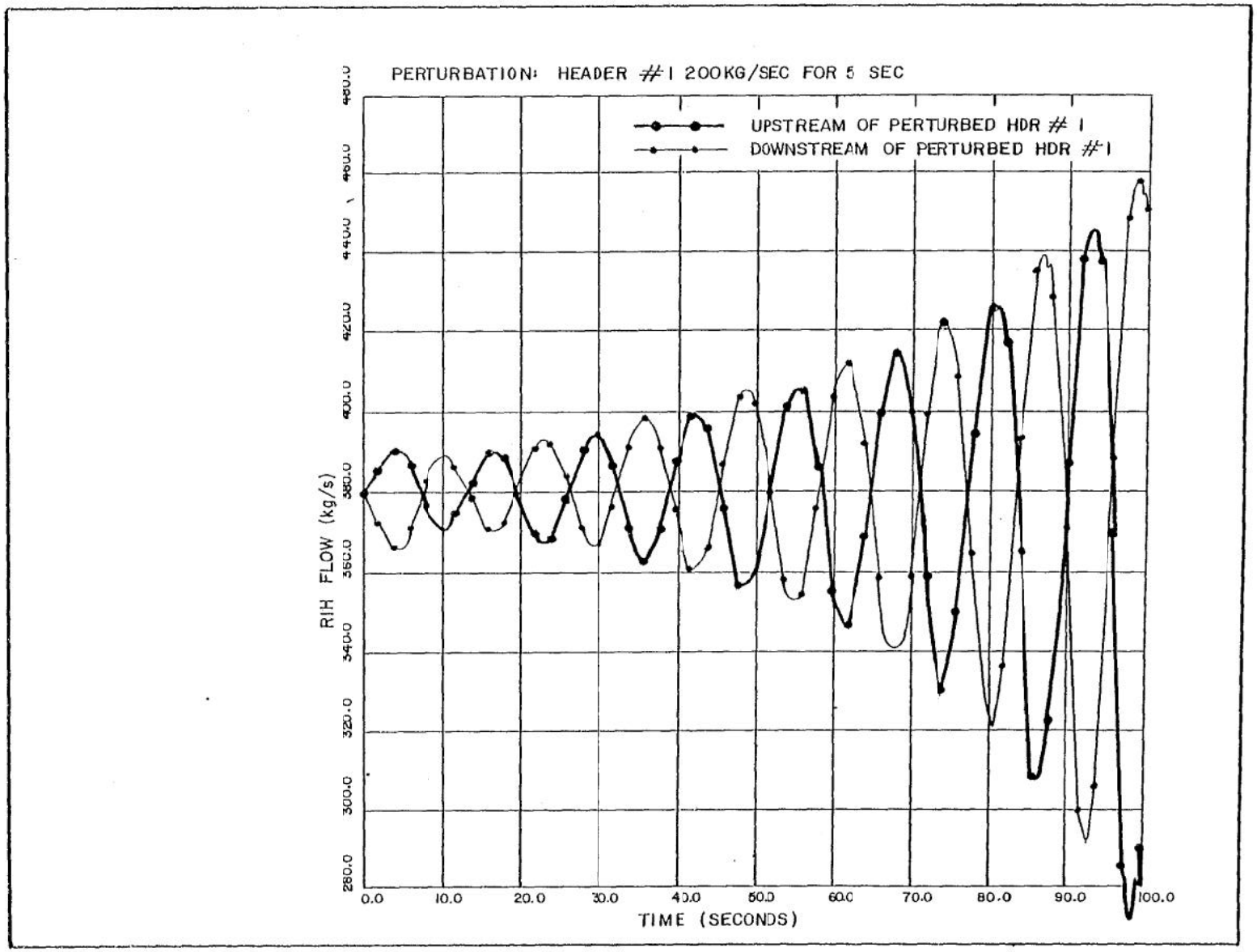

FIGURE 10 REACTOR INLET HEADER
FLOW vs. TIME, NO INTERCONNECT.

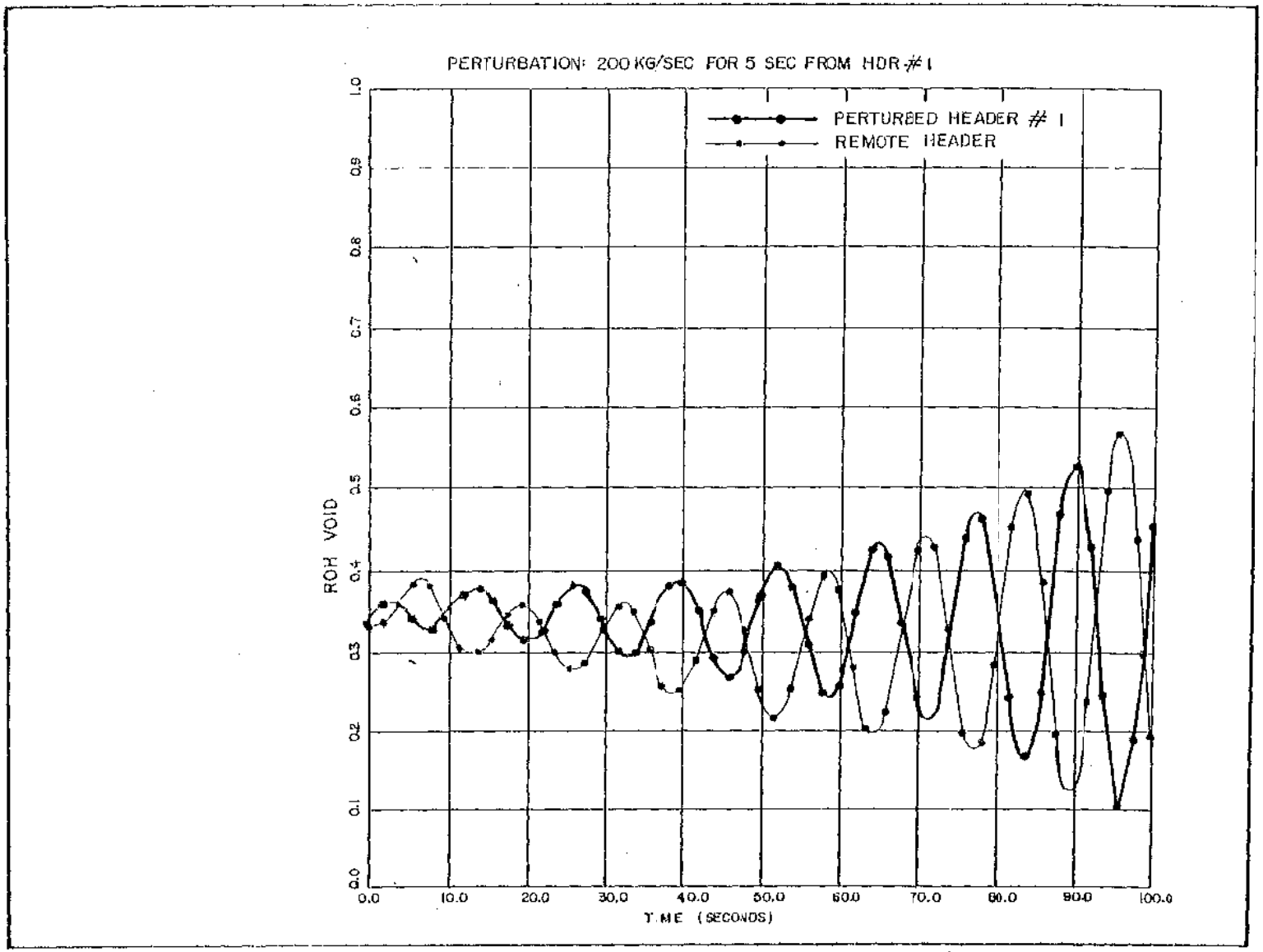

FIGURE 11 REACTOR OUTLET HEADER VOID vs TIME
NO INTERCONNECT

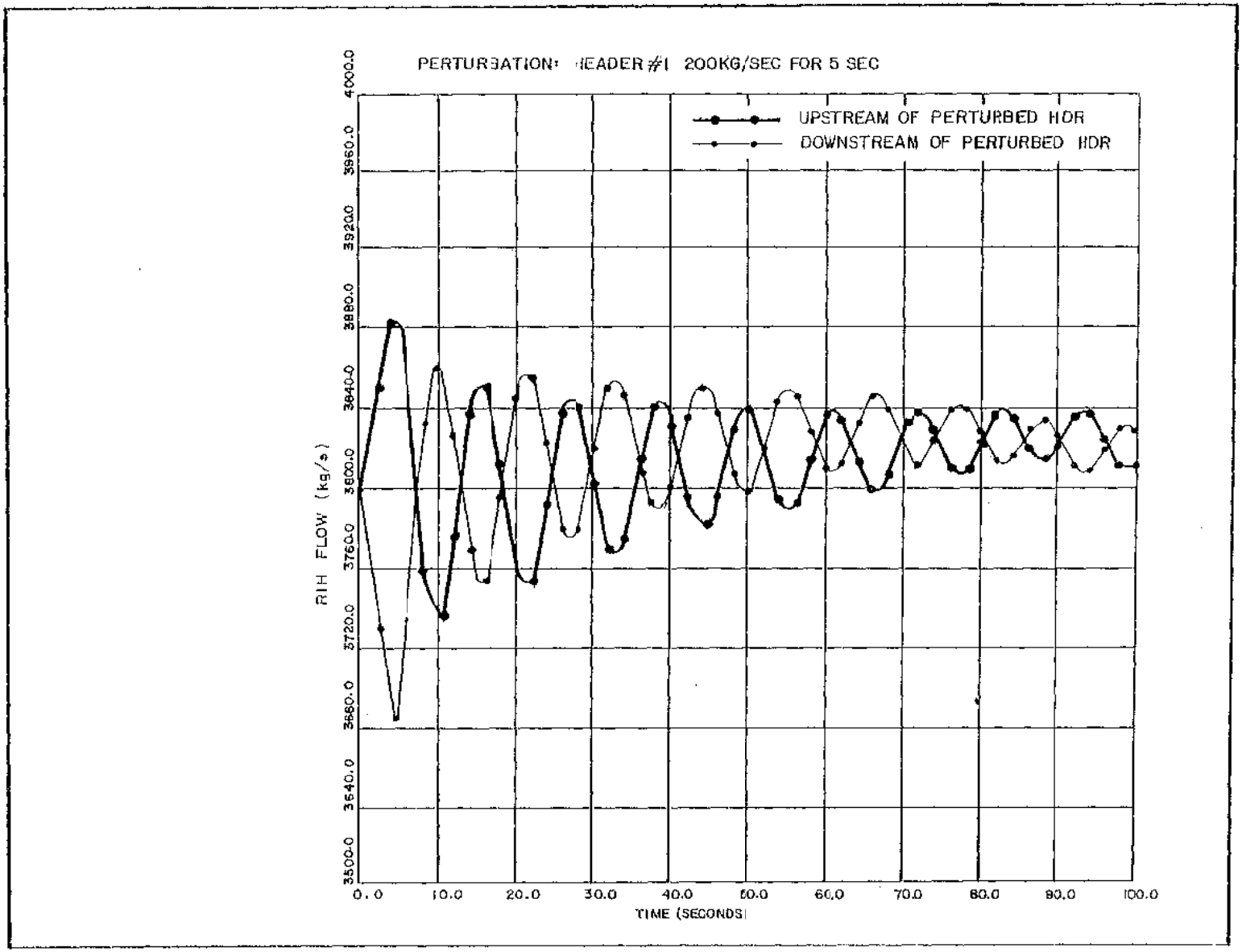

FIGURE 12 REACTOR INLET HEADER
FLOW vs. TIME, WITH INTERCONNECT, HOMOGENEOUS MODEL

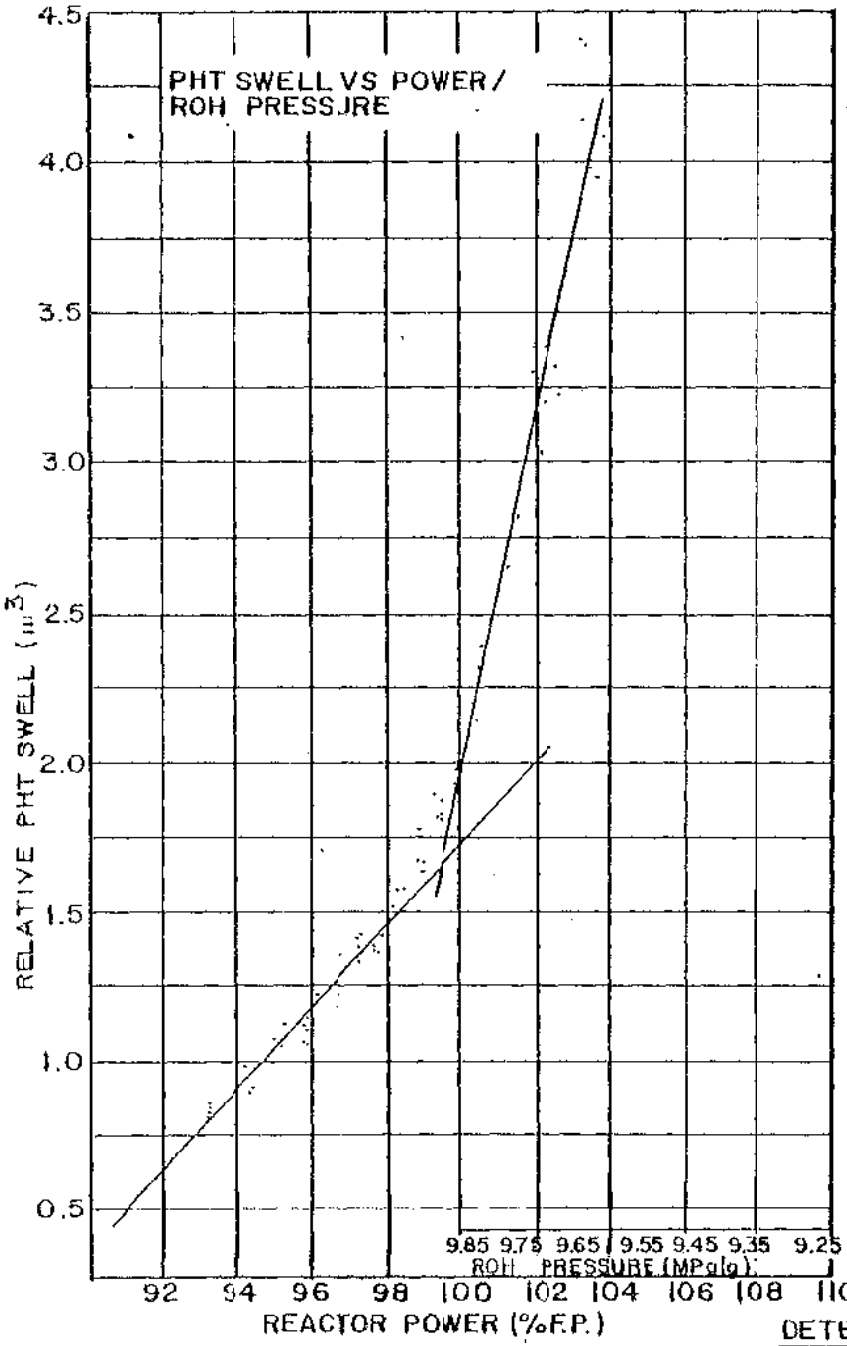

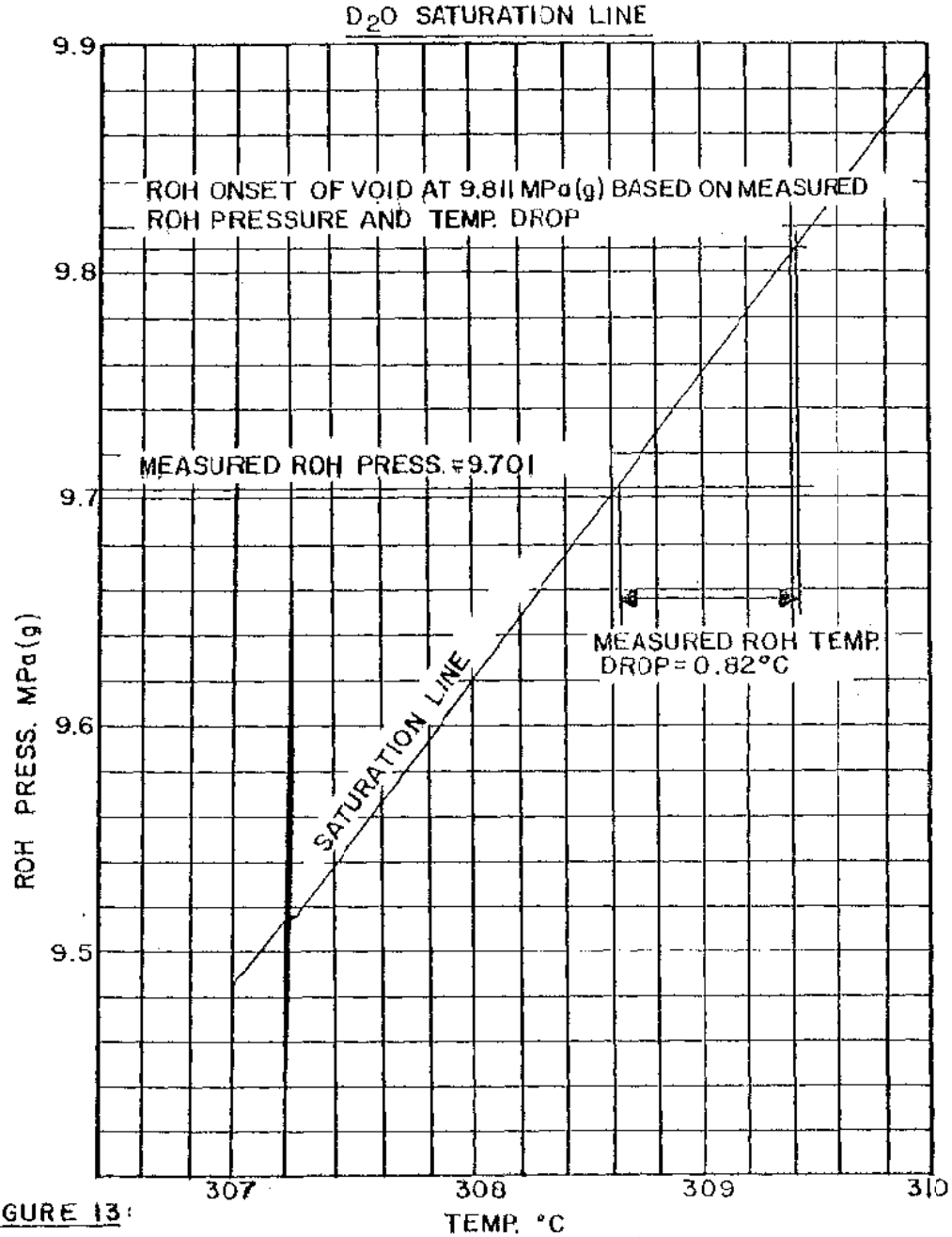

FIGURE 13: DETERMINATION OF REACTOR OUTLET HEADER PRESSURE CORRESPONDING TO ONSET OF HEADER QUALITY

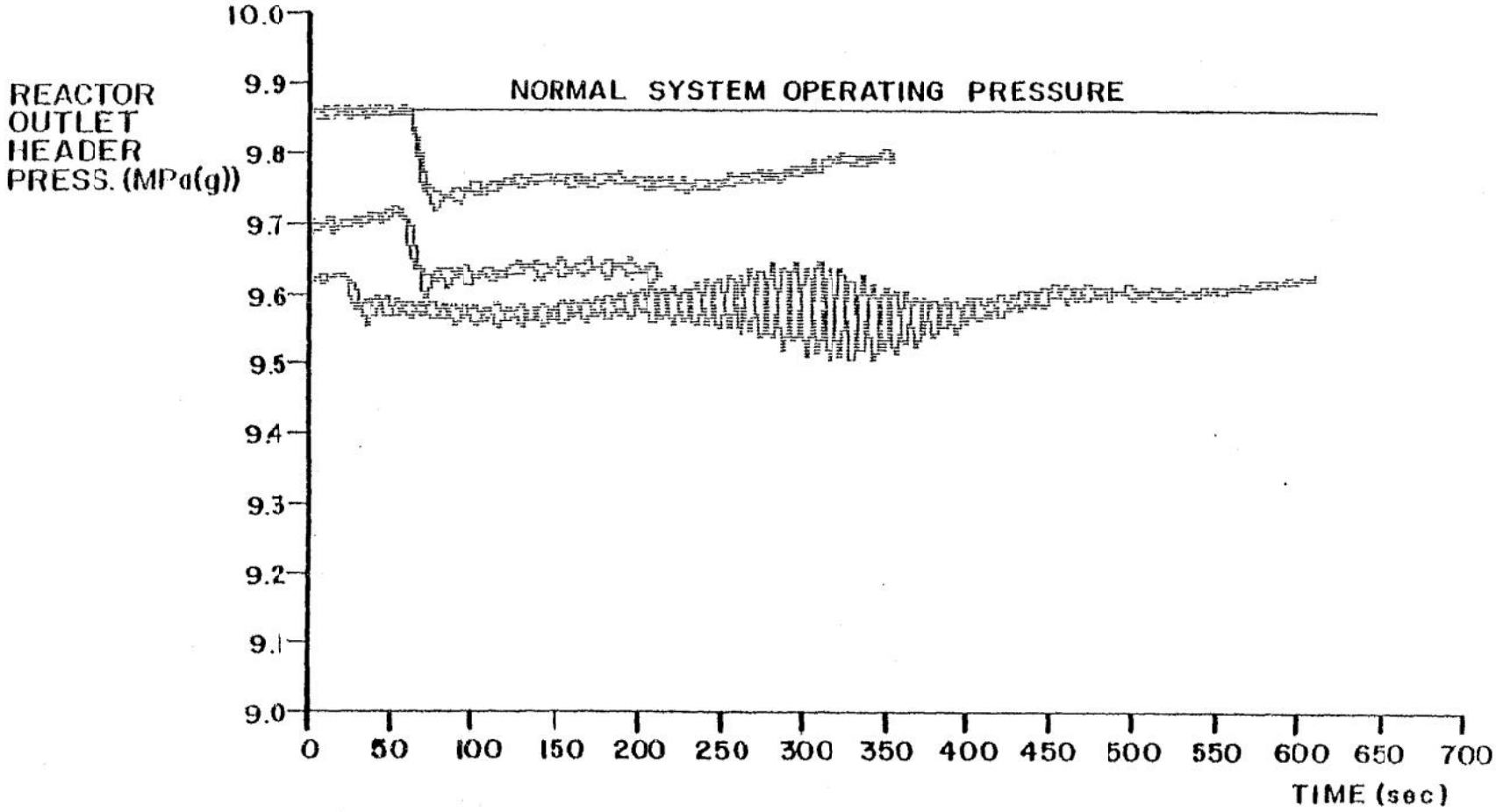

FIG.14: REACTOR OUTLET HEADER PRESS. RESPONSE TO A 10sec PRESSURIZER STEAM BLEED VALVE OPENING AT REDUCED SYSTEM OPERATING PRESS.

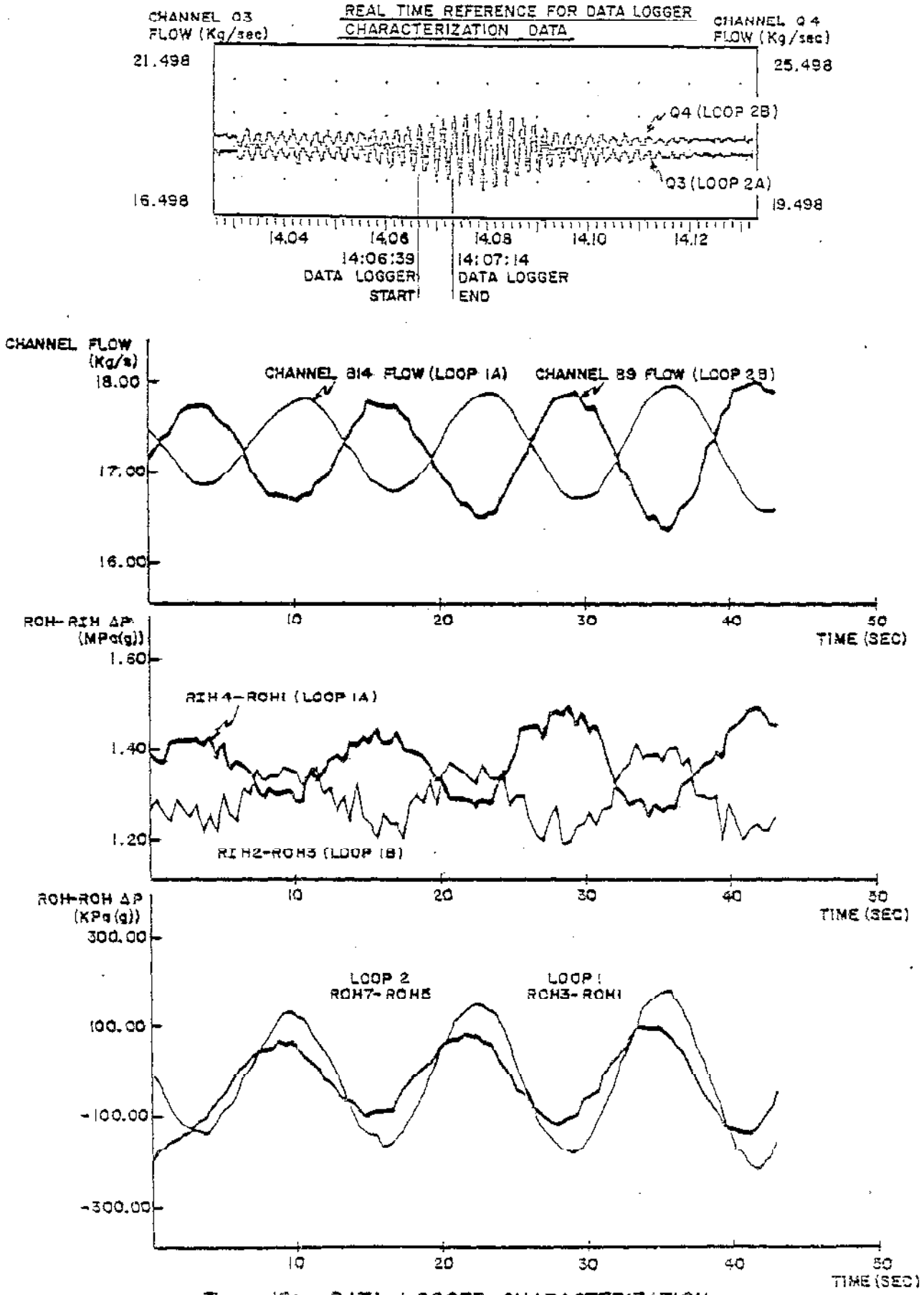

Figure 15: DATA LOGGER CHARACTERIZATION OF STABILITY PARAMETERS

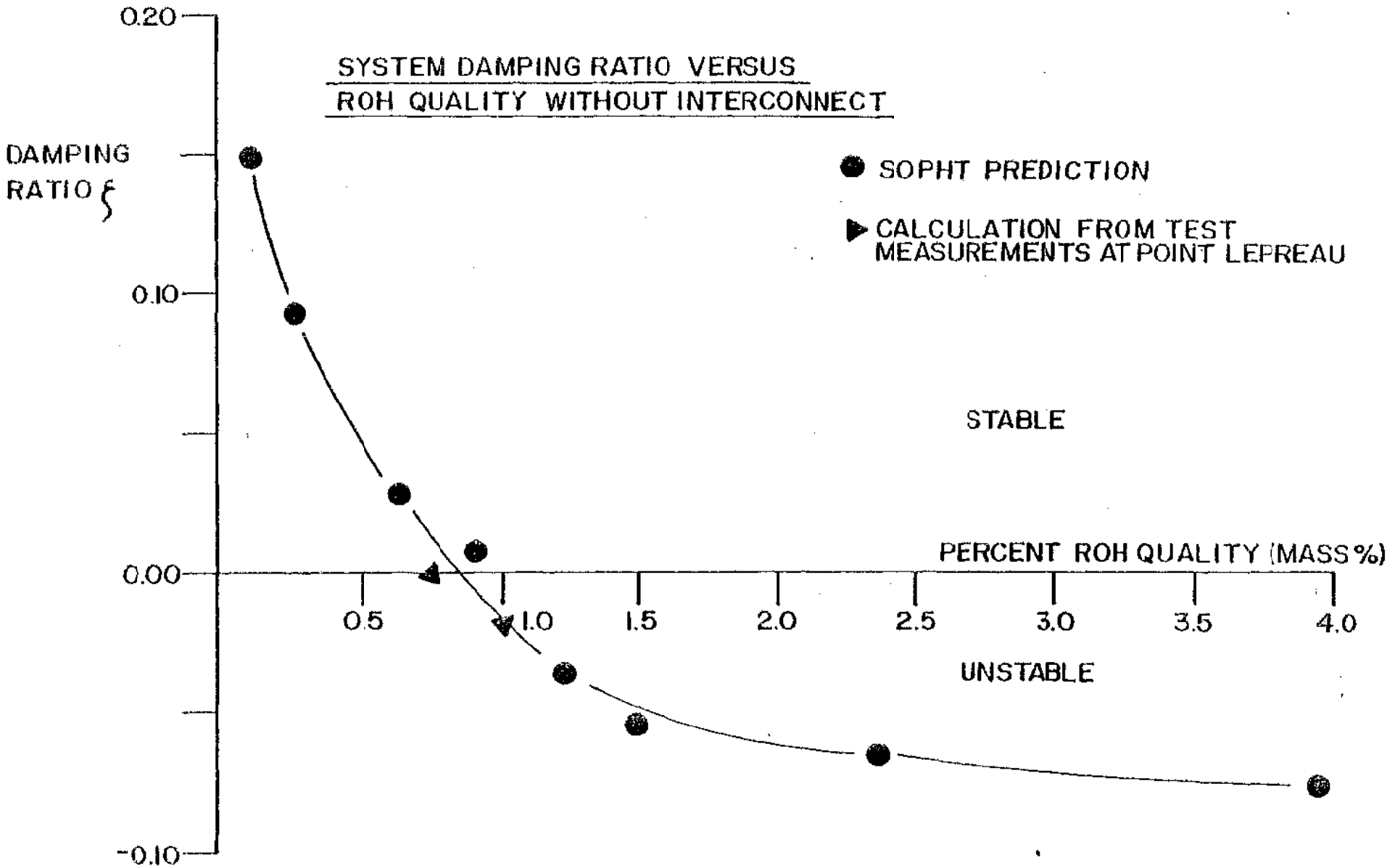

FIG. 16 : REACTOR OUTLET HEADER QUALITY ACHIEVED DURING TESTS AND SYSTEM DAMPING RATIO COMPARISON BETWEEN PREDICTION AND TEST RESULTS

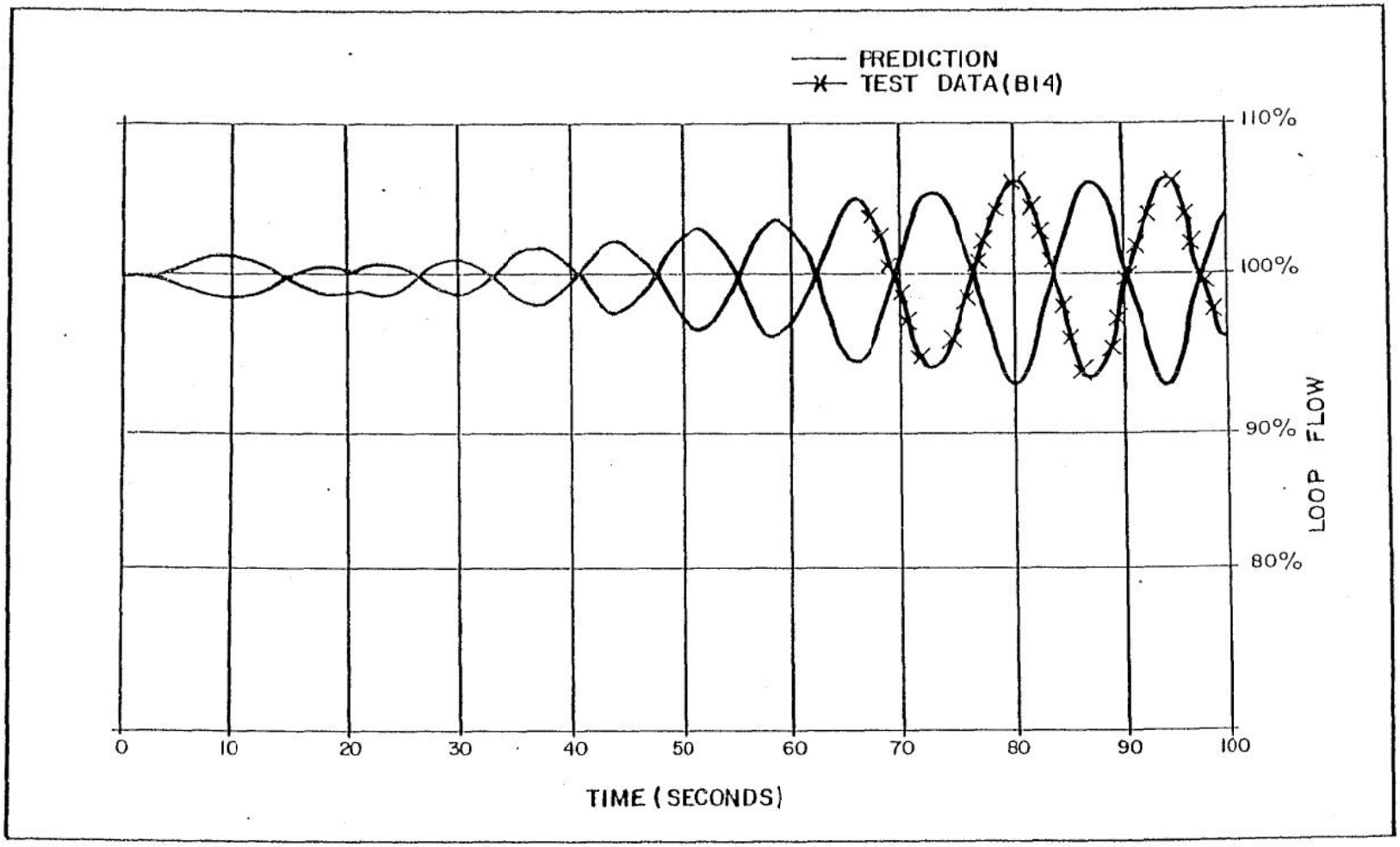

FIGURE 17: COMPARISON OF TEST DATA WITH SOPHT PREDICTION TUNED TO 65% FP DATA (5)

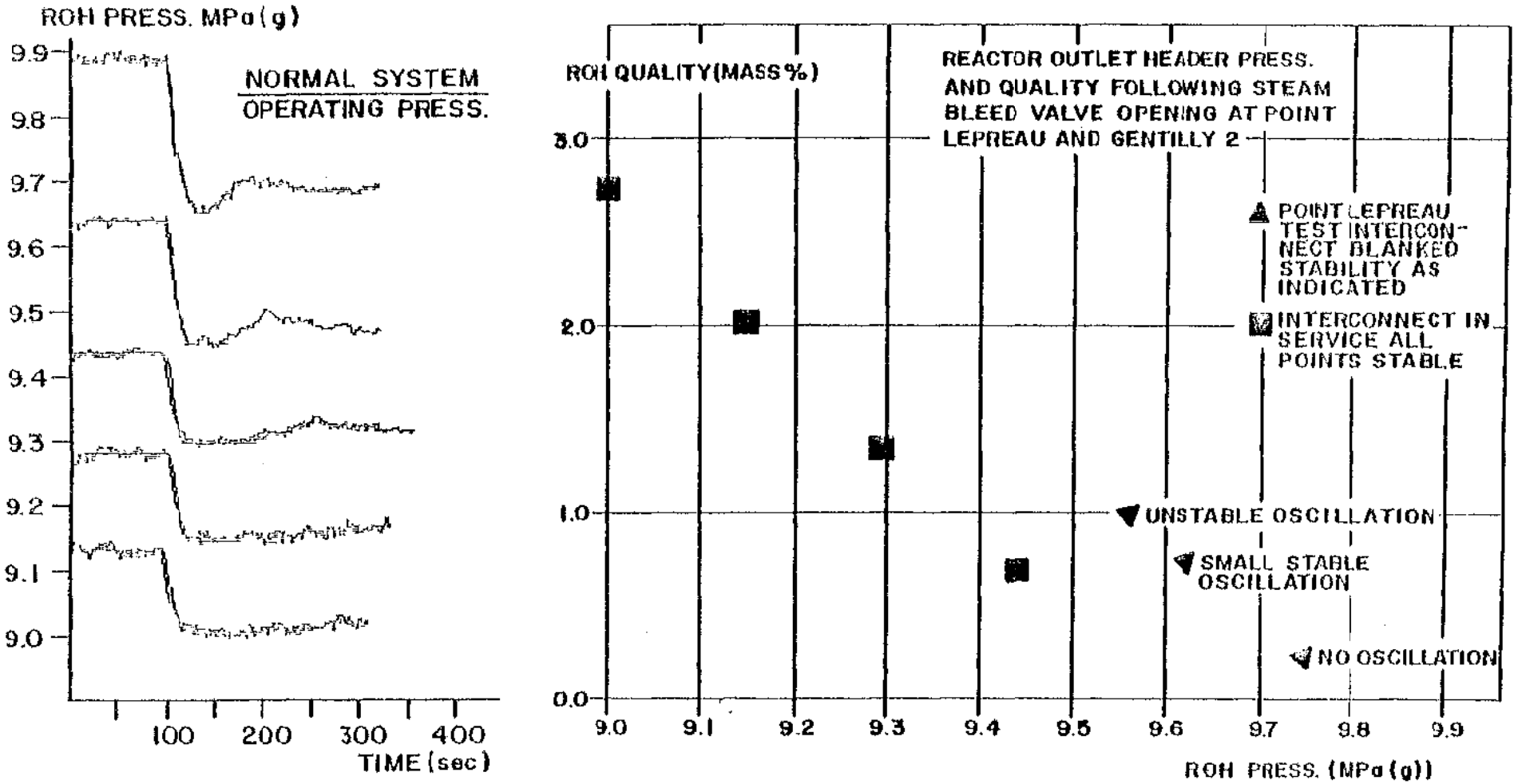

FIG. 18 : GENTILLY 2 OUTLET HEADER RESPONSE TO STEAM BLEED VALVE OPENINGS AT REDUCED PRESS. WITH INTERCONNECT PIPING IN SERVICE

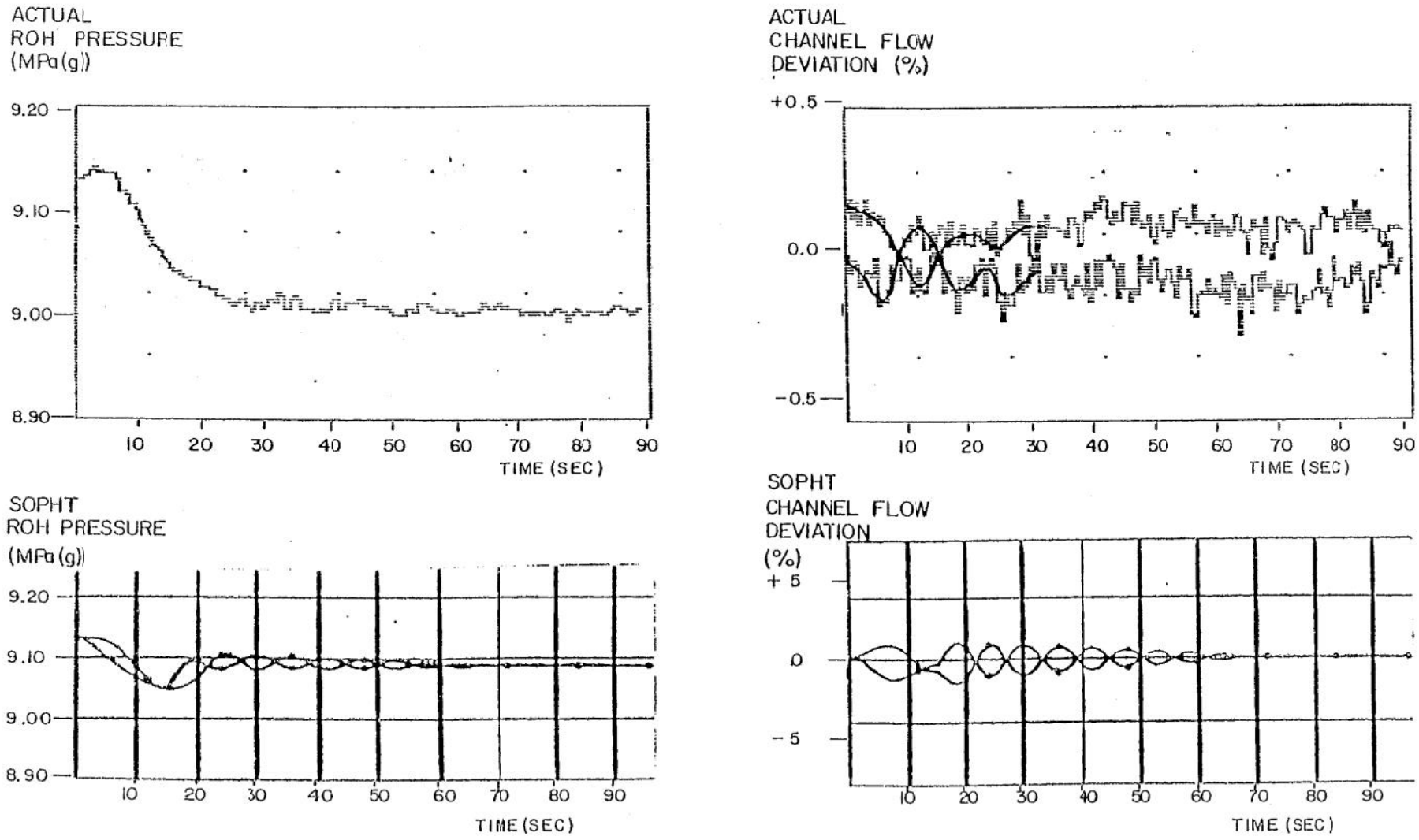

FIGURE 19: COMPARISON OF GENTILLY 2 SYSTEM RESPONSE AND SOPHT PREDICTION FOR A 10 SECOND STEAM BLEED VALVE OPENING WITH 3% ROH QUALITY